Sensors and Actuators B 230 (2016) 184–190

Contents lists available at ScienceDirect

Sensors and Actuators B: Chemical

journal homepage: www.elsevier.com/locate/snb

# High yield two-dimensional (2-D) polyaniline layer and its application in detection of B-type natriuretic peptide in human serum

Pei Liu [a], Jiyong Huang [a], David V.P. Sanchez [a], David Schwartzman [b], Seung Hee Lee [c,*], Minhee Yun [a,*]

[a] Department of Electrical and Computer Engineering, Swanson School of Engineering, University of Pittsburgh, Pittsburgh, PA 15261, United States
[b] Heart, Lung and Vascular Medicine Institute,University of Pittsburgh, Pittsburgh, PA 15261, United States
[c] Department of BIN Fusion Technology, Chonbuk National University, Jeonju 561-786, Republic of Korea

ARTICLE INFO

*Article history:*
Received 16 September 2015
Received in revised form 12 January 2016
Accepted 12 February 2016
Available online 15 February 2016

*Keywords:*
Polyaniline
Biosensor
BNP
2-D Layer

ABSTRACT

The demand for ultrasensitive and inexpensive biosensors is always strong due to increasing healthcare related concerns. Herein, we developed a simple method to prepare uniform, reliable, high yield, and low-cost two-dimensional (2-D) polyaniline layer for biosensor applications. The 2-D PANI layer's surface morphology led to a 46% increase in surface area compared to a flat 2-D surface. Due to this unique morphology and excellent semiconducting properties, the 2-D PANI layer exhibited ultrasensitive performance with excellent specificity on BNP biomarker detection in fixed Debye length condition, which is comparable to or even higher than 1-D nanostructure biosensors. In further Debye length investigation, we have observed signal changes that are varied from 8 nA to 16 nA with Debye length changes from 0.5 nm to 3.3 nm for constant BNP concentration. This result shows an improvement in device sensitivity over increasing Debye length, which conforms to Debye screening theory. With the high specificity of over 400 fold, the PANI layer was capable of monitoring significantly low BNP levels in human serum, as low as 50 pg/mL. Our findings provide an opportunity for the realization of ultrasensitive and inexpensive biosensors for clinical use.



## 1. Introduction

The most important aspect of nanostructure-based sensors is their special properties associated with their small dimensions [1,2]. As a fundamental characteristic of nanomaterials, the high surface-area-to-volume (*S*/*V*) ratio enables a number of unique physical and chemical properties such as high molecular adsorption, large surface tension force, enhanced chemical and biological activities, and large catalytic effects [1]. The nanomaterials are thus highly useful for a wide range of nanotechnology fields especially in nanoelectronics and bioelectronics [3–7] resulting in a dramatically fast growth of the sensors field. Within conventional nanosensors, 0-D (nanoparticles) and 1-D (nanotube, nanowire) nanomaterials have shown great improvements in terms of sensitivity, detection limits, and response times when compared with thin films because of their higher *S*/*V* ratio [6,7]. However, the realization of reliable 1-D nanomaterial-based biosensors is always challenging due to its fabrication complexity and lack of high-throughput production. Therefore it is of interest to develop a sensor fabrication method that enables high yield, excellent reproducibility, and ultrasensitive and highly specific detections with similar functionality to 1-D nanomaterials-based biosensors. One development would be to maintain the nanoscale thickness of the 1-D nanowire but scale up the other dimensions (e.g., length and width) to the microscale to form 2-D nanomaterials. This method becomes favorable because the 2-D nanomaterials possess high *S*/*V* ratios and good semiconducting properties, as well as offer many benefits such as good controllability and high volume production in the emerging field of large-area and low-cost electronics [8–10].

Conducting polymers are excellent biosensor materials due to their tunable conductance, the good biocompatibility, and facile surface modification [5]. While conducting polymers have been used to develop many 1-D nanostructure-based biosensors, 2-D nanostructured conducting polymers biosensors were rarely reported [11–14]. Herein, we report a novel method for the preparation of 2-D polyaniline layer combining conventional microfabrication techniques and a well-controlled chemical synthesis method [15,16]. In this study, the developed 2-D PANI layer with nanoscale thickness and microscale width were highly reproducible, and its application in field effect transistor (FET) biosensor is studied. The established method enables the fabrication of high throughput and extremely uniform PANI layer at

* Corresponding authors. Fax: +1 412 624 8003.
*E-mail addresses:* lsh1@jbnu.ac.kr (S.H. Lee), miy16@pitt.edu (M. Yun).

http://dx.doi.org/10.1016/j.snb.2016.02.051
0925-4005/

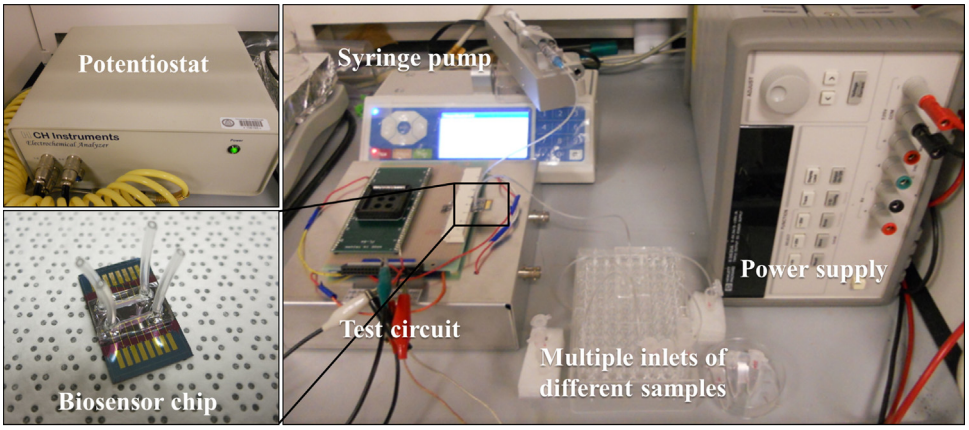


**Fig. 1.** The testing system including multiple sample inlets, a syringe pump, a chip socket, a power supply and a potentiostat.

wafer scale because of the employment of conventional CMOS (Complementary metal-oxide-semiconductor) compatible microfabrication techniques and a chemical deposition approach. The microfabrication technique defines the dimensions of the patterns with excellent controllability and the chemical deposition method allows the patterning of PANI on a wafer scale. The capability of producing high throughput and uniform PANI with high $S/V$ ratio is indeed strongly desired for sensor applications. In addition, the developed method in this study can simplify the device fabrication procedure and dramatically reduce the cost, allowing the realization of small and cheap biosensors.

One of the most significant factors that affect field-effect transistor (FET) biosensor performance is Debye screening [17] on a certain length scale, termed as Debye length ($\lambda_D$). Debye length characterizes the distance within which charges introduced by the captured molecules on the surface of PANI layer can contribute to the current change while those charges beyond the Debye length will be screened out. For aqueous solutions at room temperature, $\lambda_D$ is inversely proportional to the square root of solution ionic strength. Thus, biosensor devices a working in lower ionic strength environment should have higher sensitivity. In this study, B-type natriuretic peptide (BNP), an important cardiac marker, was used as the target for characterizing the sensing performance of the 2-D PANI layer biosensor: BNP biomarker tests were first conducted under constant Debye length environment to obtain the sensitivity and specificity of the PANI layer biosensors over detection of BNP. Debye length investigation was then carried out with constant BNP target concentration under different Debye length environment to verify the impact of Debye screening on FET sensing performance. Finally, human serum BNP tests were executed to see how the PANI layer biosensor behaves with real sample.

## 2. Experimental

### 2.1. Reagents

All chemicals were purchased from Sigma–Aldrich unless otherwise indicated. Florescence-tagged aptamer was purchased from Integrated DNA Technologies (IDT; Coralville, IA, USA). BNP aptamer and BNP biomarker (containing 32 amino acids) were purchased from Abcam. Blood samples were provided by the UPMC Heart and Vascular Institute.

### 2.2. Device fabrication and polyaniline synthesis

PANI layer were fabricated through typical lift-off process. Generally, gold/titanium electrodes were first patterned onto a 4 in wafer. After that, a bilayer structure (LOR on the bottom and photoresist on top) was patterned to serve as the template for PANI layers lift-off. A dilute polymerization method [18,19] was used to coat a uniform PANI thin film on the whole wafer. In a typical procedure, the prefabricated wafer was immersed in 180 mL of 0.5 mol/L aqueous $HClO_4$ solution. Aniline monomer (0.91 mL) was then added into the $HClO_4$ solution and stirred for 30 min at ~0–5 °C (ice bath) to form a uniform mixture. In a different beaker, the oxidant, $(NH_4)_2S_2O_8$ (APS), was dissolved in 20 mL of aqueous $HClO_4$ solution (the molar ratio of aniline/APS is 3) and cooled to ~0–5 °C. The polymerization was initiated by combining the two solutions. The mixture was stirred for 3–4 h at ~0–5 °C to accomplish the formation of PANI thin film. After the polymerization, the wafer was taken out from the solution and washed with deionized water to remove adhering PANI precipitate. After being dried in a vacuum, the PANI film coated wafer was then immersed in acetone for 5 min to remove unwanted PANI. Finally the PANI layers were obtained by cleaning the wafer with ultrasonication for a few seconds and rinsing it with deionized water 3 times. After the lift-off process, the PANI layer samples were stored for future use under vacuum conditions.

### 2.3. PANI Immobilization

The anti-BNP antibodies were covalently bonded to the PANI layers in the presence of 1-ethyl-3-(3-dimethylaminopropyl)carbodiimide (EDC) and *N*-hydroxysuccinimide (NHS). Typically, a PBS solution containing 0.1 M EDC, 0.1 M NHS, and 100 μg/mL antibody was added onto the PANI layers for 4 h at room temperature for the immobilization. The PANI layers were then thoroughly rinsed with PBS to remove physically adsorbed antibodies after the immobilization. To prevent possible nonspecific adsorption of other biomolecules to the PANI layers, PBS solution containing 200 μg/mL BSA was then dropped onto PANI layers for 30 min to block the free sites on their surface.

### 2.4. Integration of microfluidic

After monoclonal antibodies (mAbs) were functionalized onto the PANI layers surface, the polydimethylsiloxane (PDMS) microfluidics were integrated onto the sensor chip. The use of microfluidic channels is beneficial because it can reduce the environmental noise, protect the sensors, and enhance the operation safety (e.g., solution exposure). Microfluidic channels with 10 μm height, 200 μm width, and 1 mm length were placed on top

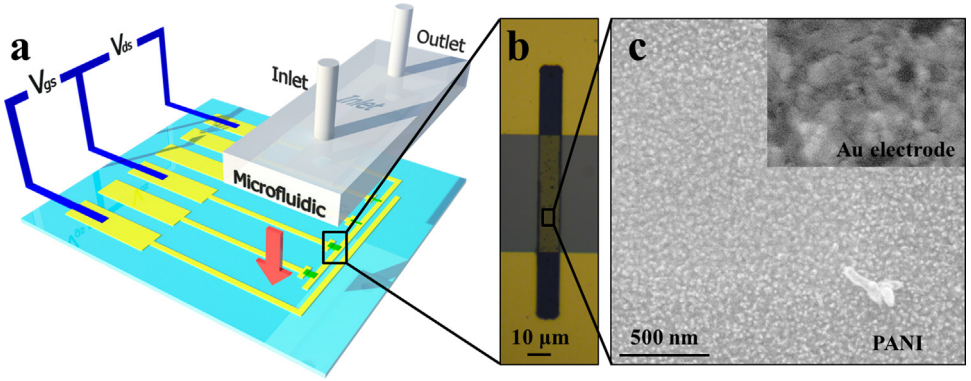


**Fig. 2.** Characterization of the PANI layer and the PANI layer FET sensor device. Schematic picture (a) of the PANI layer FET sensor device. Optical microscope image (b) of the PANI layer across Au electrodes. SEM images (c) of the PANI layer and gold electrode surface (inserted using the same scale bar) in high magnification.

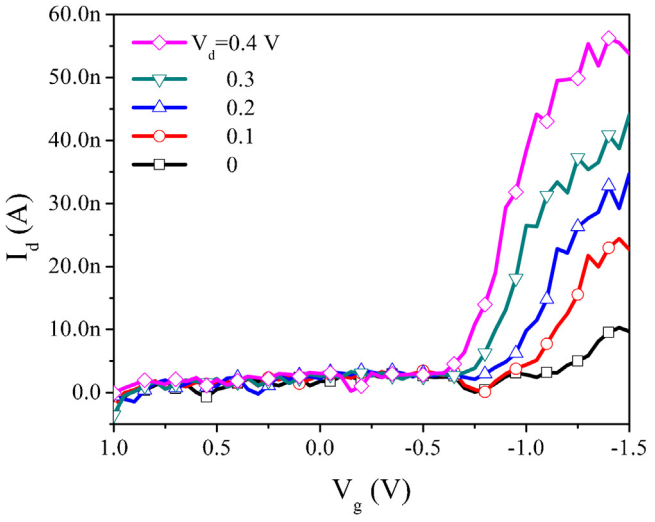


**Fig. 3.** $I_d$–$V_g$ characteristic of a 2-D PANI-NB in PBS solution: drain currents with various drain bias while sweeping gate bias.

of the PANI layers to guide the solution flow. A detailed microfluidic device integration method is available elsewhere [20].

## 3. Results and discussion

### 3.1. Characterization of the 2-D PANI layer and testing system

The configuration of the testing system is shown in Fig. 1. During the test, different samples are pumped from the multiple inlets into the microfluidic channels on the device chip by syringe pump. After the sample solution passes through the microfluidic channel, the current signal can be obtained by the potentiostat shown on the upper left of Fig. 1. The device chip shown in the lower left of Fig. 1 was designed so that it can be inserted into the socket directly and no wire-bonding steps are required. This feature ensures good contact between the socket and the chip and reduces the process steps for wire-bonding. Detailed illustrations of the PANI layer biosensor chip are shown in Fig. 2. The device is typically comprised of three electrodes as shown in Fig. 2a. A channel for controlling solution flow is created by microfluidic which is located right on top of the sensing components. Fig. 2b is an optical microscope image of the PANI layer between two Au electrodes. The dimensions of the PANI layer between the electrode is 50 μm in length by 10 μm in width by 100 nm in thickness. Close examination at high magnification reveals that the PANI surface was extremely rough (surface roughness, $R_q$ = 71.2 nm) due to formed nanomountain structures as shown in Fig. 2c. These nanomountain structures were formed during chemical synthesis and their dimension can be well-controlled [21]. In particular, additional AFM measurements showed that they have an average diameter of ~5 nm and height of ~10 nm on the PANI surface, which dramatically increases the surface area of the PANI layer by approximately 46% without changing the total volume of the 2-D structure. Another SEM image inserted in Fig. 2c reveals the surface morphology of the bare gold electrode, which clearly shows the surface roughness difference between gold and PANI. With this unique surface morphology, the total *S*/*V* ratio of the chemically developed PANI structures in this study exceeds previously grown electrochemical and CVD PANI structures [22,23], and this allows 2-D PANI layer to achieve ultra-sensitivity. The high *S*/*V* ratio and surface roughness are significantly advantageous for biosensor application because they provide multiple binding sites for proteins and enable a larger portion of the material volume to participate in binding events [24]. As a result, the 2-D PANI layer structures obtain ultrasensitive performance that is comparable to 1-D nanostructure biosensors in this study.

The detection mechanism behind the current change upon binding of target molecules for FET based amperometric biosensors can be explained by the gating effect from the surface charges introduced by the target molecules [25,26]. Because the isoelectric point (pI) of BNP used in this experiment is ~5.4 [27], the BNP molecules are negatively charged in a solution with a pH of 7.20. Therefore, the negative charges introduced by the specific binding between BNP and its receptor would lead to carrier accumulation in PANI layer, resulting in an increase in drain current [25].

The FET measurements of the 2-D PANI layer were performed using an electrolyte-gate configuration [28–30]. The drain current ($I_d$) versus gate voltage ($V_g$) characteristics of a PANI layer FET obtained as a function of different drain voltages ($V_d$) are shown in Fig. 3. The $I_d$ increased upon decreasing $V_g$ at positive drain potentials. Notably, higher drain currents can be obtained as the drain potential became more positive. The threshold voltage was about −0.6 V for the PANI layer. As the gate bias became more negative than −0.6 V, the drain currents were exponentially increased because the negative gate bias can lead to the carrier accumulation in the semiconducting channel, resulting in the conductance increase of the PANI layer. As the gate bias decreased to less than −1.2 V, the drain currents became saturated because of the "pinch-off" of the semiconducting channel. These results confirmed that the developed 2-D PANI layer is an excellent p-type material. Moreover, the drain current from the 2-D PANI layer were in the nano-amperes range which is comparable to the drain current observed from PANI nanowire-based biosensors (maximum $I_d$ was ~5 nA) tested under the same bias conditions.

FET-based biosensors with nano-scale *I–V* characteristics could be particularly sensitive if a small variation in the gate bias can lead to an observable change in the drain current without signal disturbances [29], thus enabling ultrasensitive detections. Owing to the similar surface properties and semiconducting behavior, the 2-D PANI layers are believed to have a comparable sensing performance to that of 1-D nanostructured materials.

### 3.2. PANI layer sensing performance on BNP biomarkers under constant Debye length

BNP is an important cardiac marker for the diagnosis and monitoring of heart failure [31]. This protein is elaborated from heart muscle in direct proportion to the degree of failure. Serum BNP concentration in health is ~100 pg/mL (30 pM), and may increase to greater than 2 ng/mL (600 pM) in patients with severe heart failure [32]. In this test, the sensitivity of the BNP biomarker detection was investigated without changing Debye lengths, i.e., all biomarker solutions were made with the same concentration of phosphate buffered saline (PBS) solution (0.1X). By doing this, the influence of Debye length on FET biosensor performance can be ignored. In the meantime, the specificity of the PANI layers FET biosensors was also examined with various non-specific cardiac biomarkers (Myo, cTni, and CK-MB). First, the background from the sensors was collected in PBS solution that was pumped into the microfluidic channels via a syringe pump. Then solutions containing non-specific targets were successively flowed onto the sensor. The flow into the channel was stopped during *I–V* measurements in order to eliminate the perturbations from solutions flowing across the sensor. As seen in Fig. 4a, the BNP sensor showed similar responses (within ±5%) for the PBS solution (background) and the non-specific biomarkers despite that the concentration of these non-specific biomarkers were very high (e.g., the concentration for biomarker cTni was 2 ug/mL). When the BNP biomarkers were added to the sensor through the microfluidic channel, obvious increases in the drain current were observed under the same Debye length. The response time for the biomarkers was less than 1 min in most experiments. This result revealed that the biosensor was able to specifically recognize the BNP target. More importantly, as the BNP concentration increased from 100 pg/mL to 1000 pg/mL, the drain current increased correspondingly as shown in Fig. 4a. Notable differences in the drain currents for different BNP concentrations can be observed from the figure, indicating that the sensor is capable of distinguishing different BNP levels in solution.

Sensor test results can be influenced by factors associated with both the sensor and the test conditions. Hence, we tested 20 devices to reduce the uncertainty within our experiments and increased the confidence in our results. These devices were tested with all five different BNP concentrations without changing Debye length as well. The response changes were calculated with respect to the device responses recorded using PBS as the background/reference value. All the data for different BNP concentrations were statistically analyzed and the results are plotted in Fig. 4b. The horizontal bars are the median of each point. The vertical bars show the response ranges for each point with 80% confidence, in which the mean of the data is located at the center. The sensors showed considerable responses to different BNP levels. For example, average changes of about 22%, 40%, 65%, 88%, and 98% were achieved for the BNP concentrations of 50 pg/mL, 100 pg/mL, 200 pg/mL, 500 pg/mL, and 1000 pg/mL, respectively. Fig. 4b shows that initial ΔI/I responses increase significantly with increased BNP concentrations from 50 to 200 pg/mL, and then the slope of the responses decreased with higher BNP concentration due to the saturation of available antibody sites. Remarkably, the cut-off concentration for BNP in blood is about 100 pg/mL, which 1) falls directly in the linear detection range of our PANI layer sensors and 2) confirms that the sensor can detect medically relevant changes (i.e., <100 pg/mL) in BNP concentration.

Fig. 4b also displays the 80% confidence interval for the samples recorded for each concentration and the point on each bar highlights the median value. While the confidence intervals overlap for some of the concentrations tested, the clear differences between the mean (centers of the intervals) and median better highlight the distribution of the data across all our results. Hence the medians in the graph are relatively more useful references for the test results. As shown in the figure, the range of 80% confidence interval widened with an increase of the BNP concentration. This is believed to be due mainly to the accumulative interference among the bound BNP targets on the surface because more BNP can be captured by the sensor at higher BNP concentrations. This would possibly lead to appreciable variations in the sensor current changes. The information of reaction dissociation constant for the coupling of BNP and its receptor can be extracted from Fig. 4b, which is highly useful for the quantification of BNP concentrations.

### 3.3. Debye length investigation

To study the impact of the solution Debye length to the PANI FET sensor performance, five PBS dilutions contained constant concentration of BNP were tested for the BNP detection. Larger $I_d$ changes can be observed in 0.05x PBS than that in 0.5x PBS. For instance, the $I_d$ changes of the FET sensor in 0.05x and 0.5x PBS solutions were 15.7 nA and 10.9 nA at $V_d$ = 0.7 V as shown in Fig. 5b. The ionic strengths of 0.05x and 0.5x PBS solutions yielded Debye lengths of 3.3 nm and 1.04 nm, respectively. Because of the larger $\lambda_D$ in 0.05x PBS, more charges carried by the BNP molecules were effective in altering the conductivity of the PANI layer, resulting in a larger $I_d$ changes. From Fig. 5a, we also observed that background current signals of PBS solutions without BNP biomarkers (▲ 0.5x PBS and ● 0.05x PBS in Fig. 5a) decreased with increasing of Debye length. Since the sensitivity is defined as $\Delta I_d/I_d$, when Debye length increases, $I_d$ decreases and $\Delta I_d$ increases. Therefore, the overall sensitivity improves. This result indicates that the sensitivity of the PANI FET biosensor can be greatly improved by increasing the Debye length. Fig. 5b shows the $I_d$ changes versus the solution Debye length at $V_d$ = 0.7 V and $V_g$ = −0.25 V. An increase in $\Delta I_d$ can be observed as the Debye screen length increases. Further nonlinear fitting (red dash line in Fig. 5b) shows an exponential-like curve with the largest measured current change at 16 nA under 3.3 nm Debye length. The change of drain current $\Delta I_d$ will be saturated and reach a maximum value around 18 nA with a further increase in Debye length (going right along the red dash curve). This maximum current change occurs when all surface bound charges are kept within Debye length. Hence, all charges are contributing to gating the sensing component. This also confirms that the increase of Debye length can enhance the FET sensing performance.

### 3.4. PANI layers sensing performance on human serum

The detection of BNP in whole blood can be complicated by the precipitation of red blood cells onto the PANI layer surfaces which would block the BNP antibodies on the sensor surface from binding to the BNP targets. This can significantly affect the response from the sensor. Therefore, human serum samples were tested instead to demonstrate the feasibility of the biosensor. Serum samples from patients with heart failure were obtained after separating the red blood cells from the whole blood by centrifugation (Fisher Scietific accuSpin 400, 3000 rpm for 10 min). As shown in Fig. 6, a total of three serum samples were tested from subjects with unknown BNP concentrations. Notably, the sample UPDS1024_SR03 showed the greatest response and UPDS1020_NR01 had the least response among these three samples. Referring to sample UPDS1020_NR01,

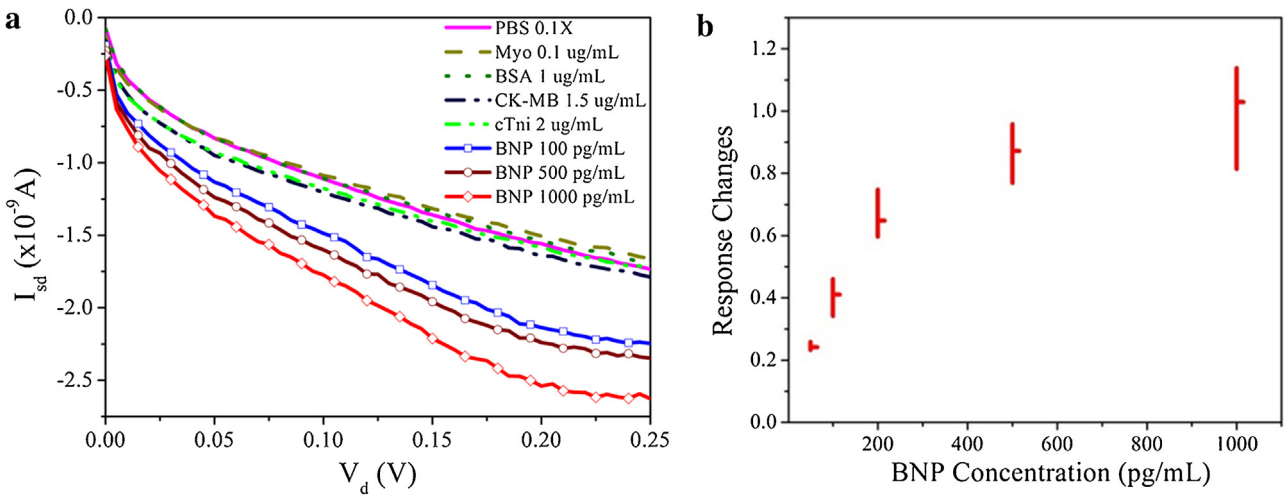


**Fig. 4.** Test results of the PANI layer FET sensors for BNP in PBS solution. Specificity tests results (a) of the PANI layer FET biosensors. Normalized response versus concentration of BNP (b).

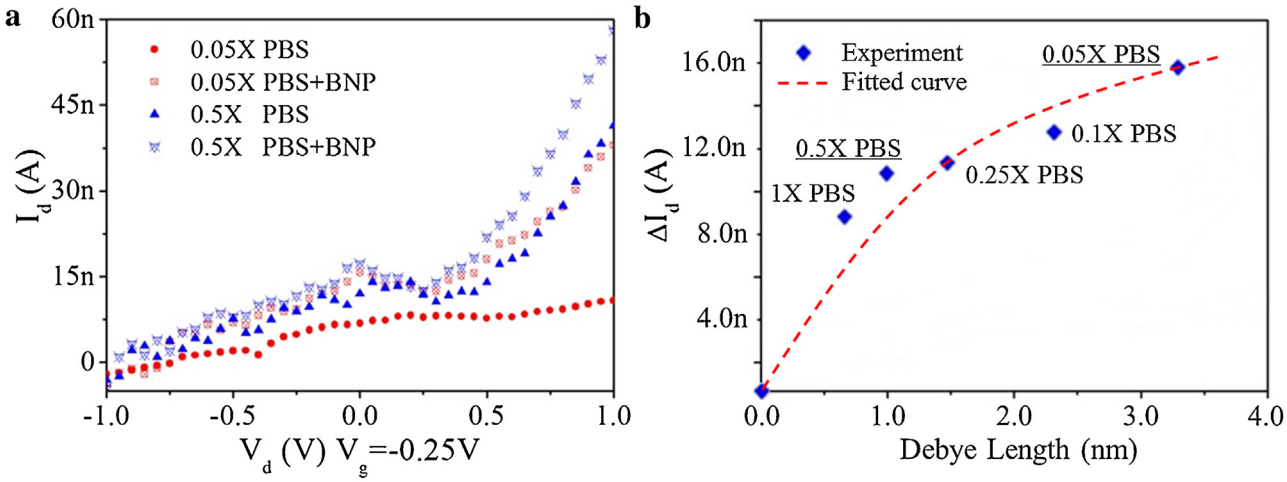


**Fig. 5.** $I_d$–$V_d$ curves (a) of a PANI-NB-FET sensor in different PBS dilutions. Drain current change as a function of solution Debye length, and the nonlinear fitting of current change versus Debye length (b). Within shorter Debye length, more of the charges carried by the target molecules will be screened out by counter ions. (For interpretation of the references to color in the text, the reader is referred to the web version of this article.)

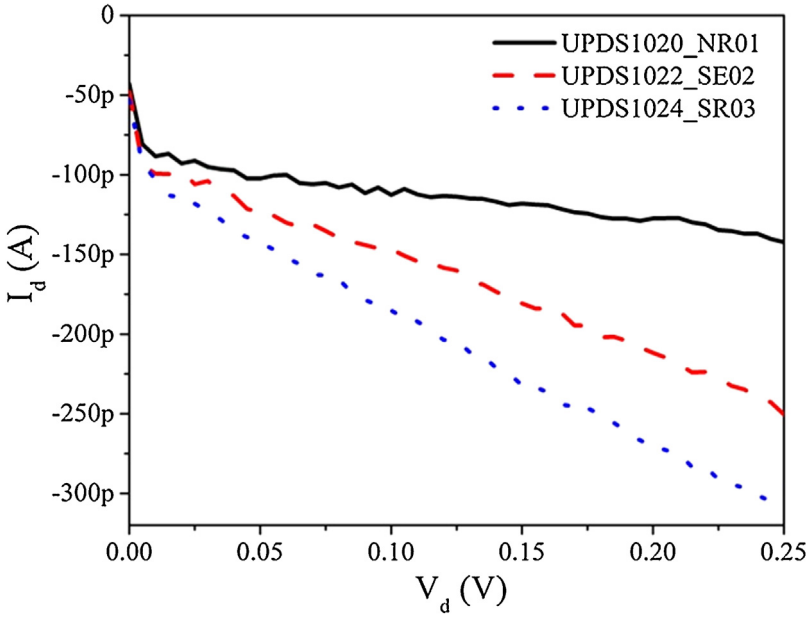


**Fig. 6.** The PANI layer FET sensor responses to human serum sample.

sample UPDS1022_SE02 and sample UPDS1024_SR03 exhibited ~72.4% and ~113.8% greater in the drain current. These test results reveal that the BNP level in these samples is in the order of UPDS1024_SR03 > UPDS1022_SE02 > UPDS1020_NR01. After the sensing tests, the BNP concentrations were quantified using ELISA test kits. The results suggest that UPDS1020_NR01 was collected from a healthy person without any heart diseases (< 100 pg/mL). And according to the ELISA test, the BNP level in UPDS1022_SE02 and UPDS1024_SR03 was ~129 pg/mL and ~293 pg/mL. This is consistent with the measurement results from the PANI layer sensors, indicating the feasibility of using the PANI layer FET sensors to approximately monitor BNP levels in serum. However, it is important to note that different serum samples have distinct ionic strength, i.e., distinct Debye length. Larger ionic strength will result in higher drain-source current as shown in Fig. 5a, while different Debye length also causes variety in current signal changes. These issues can explain the inconsistency between quantitative results in biomarkers and real serum samples tests. Hence, accurately quantifying the target concentration in human serum samples is challenging and requires future work. In summary of human serum experiment, we could conclude in this research that 2-D PANI based FET biosensor has shown the ability to quantify the BNP biomarkers and the potential for biosensor applications.

## 4. Conclusions

We have established a simple way to develop 2-D PANI layer biosensors that exhibit extremely high specificity and sensitivity. Debye length study also shows expected FET sensing performance under different concentration of PBS. The 2-D PANI layer possessed similar surface profiles and FET behavior as 1-D nanowires, thus confirming the similarities in sensor performance. Additionally, the BNP detections in serum with the PANI layer sensors reveal that the sensors are highly specific and sensitive. This demonstration of monitoring BNP in serum provides great promise and low-cost sensor devices for clinical use.

## Acknowledgements

The authors are grateful for financial support from the National Science Foundation (NSF ECCS 0824035), and the National Institute of Health (NIH 1R21 EB008825). P. Liu and J. Huang equally contributed to this work. Minhee Yun acknowledges Brian Korea Plus, and SH Lee acknowledges the support from LG Yonam Foundation.

## Appendix A. Supplementary data

Supplementary data associated with this article can be found, in the online version, at http://dx.doi.org/10.1016/j.snb.2016.02.051.

## References

[1] E. Roduner, Size matters: why nanomaterials are different, Chem. Soc. Rev. 35 (2006) 583–592.
[2] C.N.R. Rao, A.K. Cheetham, Science and technology of nanomaterials: current status and future prospects, J. Mater. Chem. 11 (2001) 2887–2894.
[3] J. Wang, M. Musameh, Y.H. Lin, Solubilization of carbon nanotubes by nafion toward the preparation of amperometric biosensors, J. Am. Chem. Soc. 125 (2003) 2408–2409.
[4] R.J. Chen, S. Bangsaruntip, K.A. Drouvalakis, N.W.S. Kam, M. Shim, Y.M. Li, W. Kim, P.J. Utz, H.J. Dai, Noncovalent functionalization of carbon nanotubes for highly specific electronic biosensors, Proc. Natl. Acad. Sci. U. S. A. 100 (2003) 4984–4989.
[5] M. Gerard, A. Chaubey, B.D. Malhotra, Application of conducting polymers to biosensors, Biosens. Bioelectron. 17 (2002) 345–359.
[6] X.L. Luo, A. Morrin, A.J. Killard, M.R. Smyth, Application of nanoparticles in electrochemical sensors and biosensors, Electroanalysis 18 (2006) 319–326.
[7] F. Patolsky, G.F. Zheng, C.M. Lieber, Nanowire-based biosensors, Anal. Chem. 78 (2006) 4260–4269.
[8] H.W. Yan, Y.L. Yang, Z.P. Fu, B.F. Yang, L.S. Xia, S.Q. Fu, F.Q. Li, Fabrication of 2D and 3D ordered porous ZnO films using 3D opal templates by electrodeposition, Electrochem. Commun. 7 (2005) 1117–1121.
[9] R. Gunawidjaja, C.Y. Jiang, S. Peleshanko, M. Ornatska, S. Singamaneni, V.V. Tsukruk, Flexible and robust 2D arrays of silver nanowires encapsulated within freestanding layer-by-layer films, Adv. Funct. Mater. 16 (2006) 2024–2034.
[10] W.R. Yang, K.R. Ratinac, S.P. Ringer, P. Thordarson, J.J. Gooding, F. Braet, Carbon nanomaterials in biosensors: should you use nanotubes or graphene? Angew. Chem. Int. Ed. 49 (2010) 2114–2138.
[11] M. Lin, M. Cho, W.S. Choe, J.B. Yoo, Y. Lee, Polypyrrole nanowire modified with Gly-Gly-His tripeptide for electrochemical detection of copper ion, Biosens. Bioelectron. 26 (2010) 940–945.
[12] J.Y. Huang, X.L. Luo, I. Lee, Y.S. Hu, X.T. Cui, M.H. Yun, Rapid real-time electrical detection of proteins using single conducting polymer nanowire-based microfluidic aptasensor, Biosens. Bioelectron. 30 (2011) 306–309.
[13] C. Garcia-Aljaro, M.A. Bangar, E. Baldrich, F.J. Munoz, A. Mulchandani, Conducting polymer nanowire-based chemiresistive biosensor for the detection of bacterial spores, Biosens. Bioelectron. 25 (2010) 2309–2312.
[14] Y.W. Xu, H.J. Lee, Y.S. Hu, J.Y. Huang, S.W. Kim, M.H. Yun, Detection and identification of breast cancer volatile organic compounds biomarkers using highly-sensitive single nanowire array on a chip, J. Biomed. Nanotechnol. 9 (2013) 1164–1172.
[15] J. Janata, M. Josowicz, Conducting polymers in electronic chemical sensors, Nat. Mater. 2 (2003) 19–24.
[16] A. Malinauskas, Chemical deposition of conducting polymers, Polymer 42 (2001) 3957–3972.
[17] E. Stern, R. Wagner, F.J. Sigworth, R. Breaker, T.M. Fahmy, M.A. Reed, Importance of the Debye screening length on nanowire field effect transistor sensors, Nano Lett. 7 (2007) 3405–3409.
[18] N.R. Chiou, C.M. Lui, J.J. Guan, L.J. Lee, A.J. Epstein, Growth and alignment of polyaniline nanofibres with superhydrophobic, superhydrophilic and other properties, Nat. Nanotechnol. 2 (2007) 354–357.
[19] J.J. Xu, K. Wang, S.Z. Zu, B.H. Han, Z.X. Wei, Hierarchical nanocomposites of polyaniline nanowire arrays on graphene oxide sheets with synergistic effect for energy storage, ACS Nano 4 (2010) 5019–5026.
[20] J.Y. Huang, I. Lee, X.L. Luo, X.T. Cui, M.H. Yun, Shadow masking for nanomaterial-based biosensors incorporated with a microfluidic device, Biomed. Microdevices 15 (2013) 531–537.
[21] J. Stejskal, I. Sapurina, J. Prokes, J. Zemek, In-situ polymerized polyaniline films, Synth. Met. 105 (1999) 195–202.
[22] I. Lee, X. Luo, X.T. Cui, M. Yun, Highly sensitive single polyaniline nanowire biosensor for the detection of immunoglobulin G and myoglobin, Biosens. Bioelectron. 26 (2011) 3297–3302.
[23] Y. Hu, D. Perello, U. Mushtaq, M. Yun, A single palladium nanowire via electrophoresis deposition used as a ultrasensitive hydrogen sensor, IEEE Trans. Nanotechnol. 7 (2008) 693–699.
[24] K. Rechendorff, M.B. Hovgaard, M. Foss, V.P. Zhdanov, F. Besenbacher, Enhancement of protein adsorption induced by surface roughness, Langmuir 22 (2006) 10885–10888.
[25] X.P.A. Gao, G.F. Zheng, C.M. Lieber, Subthreshold regime has the optimal sensitivity for nanowire FET biosensors, Nano Lett. 10 (2010) 547–552.
[26] T. Uno, H. Tabata, T. Kawai, Peptide-nucleic acid-modified ion-sensitive field-effect transistor-based biosensor for direct detection of DNA hybridization, Anal. Chem. 79 (2007) 52–59.
[27] R.L. Gundry, J.E. Van Eyk, Unraveling the complexity of circulating forms of brain natriuretic peptide, Clin. Chem. 53 (2007) 1181–1182.
[28] A.S. Dhoot, J.D. Yuen, M. Heeney, I. McCulloch, D. Moses, A.J. Heeger, Beyond the metal-insulator transition in polymer electrolyte gated polymer field-effect transistors, Proc. Natl. Acad. Sci. U. S. A. 103 (2006) 11834–11837.
[29] M.M. Alam, J. Wang, Y.Y. Guo, S.P. Lee, H.R. Tseng, Electrolyte-gated transistors based on conducting polymer nanowire junction arrays, J. Phys. Chem. B 109 (2005) 12777–12784.
[30] J. Zaumseil, X.N. Ho, J.R. Guest, G.P. Wiederrecht, J.A. Rogers, Electroluminescence from electrolyte-gated carbon nanotube field-effect transistors, ACS Nano 3 (2009) 2225–2234.
[31] T.J. Wang, M.G. Larson, D. Levy, E.J. Benjamin, E.P. Leip, T. Omland, P.A. Wolf, R.S. Vasan, Plasma natriuretic peptide levels and the risk of cardiovascular events and death, N. Engl. J. Med. 350 (2004) 655–663.
[32] A.S. Maisel, P. Krishnaswamy, R.M. Nowak, J. McCord, J.E. Hollander, P. Duc, T. Omland, A.B. Storrow, W.T. Abraham, A.H.B. Wu, P. Clopton, P.G. Steg, A. Westheim, C.W. Knudsen, A. Perez, R. Kazanegra, H.C. Herrmann, P.A. McCullough, Rapid measurement of B-type natriuretic peptide in the emergency diagnosis of heart failure, N. Engl. J. Med. 347 (2002) 161–167.

## Biographies

**Pei Liu** received his B.S. in Material Physics from Nanjing University, Nanjing, China in 2011. He is currently pursuing his Ph.D. degree in Electrical Engineering at University of Pittsburgh. His research interesting includes polyaniline based flexible and stretchable biosensors and polyaniline nanostructure synthesis.

**Jiyong Huang** obtained his B.S. and M.S. from the Beijing University of Chemical Technology. He recieved his Ph.D. in 2014 from the University of Pittsburgh. His research interests are nanoscale electronics and their application in sensors.

**David V. P. Sanchez** is an Assistant Professor in the Dept. Of Civil and Environmental Engineering and the Assistant Director for the Mascaro Center for Sustainable Innovation at the University of Pittsburgh where he received his Ph.D. in 2014. His research interests include bioelectrochemical material applications for energy and water sustainability.

**David Schwartzman** is a Professor of Medicine at the University of Pittsburgh School of Medicine and a member of the UPMC Cardiovascular Institute and the UPMC Center for Atrial Fibrillation. Dr. Schwartzman obtained his M.D. from New York University and completed his residency here as well as two Fellowships, one in Cardiology and a second in Interventional Cardiology. He continued his training with two more Fellowships at the University of Pennsylvania, one in Electrophysiology and a second in Electrophysiology Research. Dr. Schwartzman is a Fellow of the American College of Cardiology, the American Heart Association, and the Heart Rhythm Society.

**Seung Hee Lee** is a Professor in the Department of Bio-Information-Nanotechnology (BIN) Convergence Technology at Chonbuk National University in Korea. He received his Ph.D. from Kent State University in 1994. His research interests include liquid crystals for display devices and biosensors suitable for smart phones

**Minhee Yun** holds Ph. D. degree from Arizona State University in 1998 and is an associate professor of electrical and computer engineering after four years as a senior staff in the device application group at the Jet Propulsion Laboratory in Pasadena, CA. While at JPL, he led research efforts in the area of device fabrication based on MEMS technologies, and chemical and biochemical nanowire sensor arrays for life detection on Mars and bio-signature detection of emerging diseases. His current research interests include the development of nano-electronic devices for bio-medical applications for early detection of disease signatures using nano-structured materials.